An Uncertainty Analysis of Downward Pressure Applied to the Wafer Based on a Flexible Airbag by a Double Side Polishing Machine

KOU Minghu, ZHOU Huiyan, HAO Yuanlong, LV Yue, JIANG Jile*

(*Beijing TSD Semiconductor Equipment Co., Ltd. Beijing 101300*)

Abstract: The process of wafer polishing is known to be highly demanding, and even small deviations in the processing parameters can have a significant impact on the quality of the wafers obtained. During the process of wafer polishing, maintaining a constant pressure value applied by the polishing head is essential to achieve the desired flatness of the wafer. The accuracy of the downward pressure output by the polishing head is a crucial factor in producing flat wafers. In this paper, the uncertainty component of downward pressure is calculated and its measurement uncertainty is evaluated, and a method for calculating downward pressure uncertainty traceable to international basic unit is established. Therefore, the reliability of double side polishing machine has been significantly improved.

Keywords: Downward Pressure, Uncertainty, Traceable, Polishing, Wafer

1 Introduction

In light of the swift advancements in semiconductor technology and information industry, the integration of semiconductor chips has become increasingly vital. This is especially emphasized by the escalated requirements for flatness and roughness of these semiconductor chips in both social production and daily life[1]. Grinding, etching and polishing are important processes to ensure the integrity and flatness of wafer surface. Polishing refers to the machining process of improving micro defects on the surface of a single crystal silicon wafer to achieve extremely high flatness and minimal surface roughness values. The surface should be free from any metamorphic layer or scratches[2]. During the polishing process, the wafer is pressed onto the polishing pad by the polishing head, and then rotated by a polishing disk. The wafer is then flattened using a combination of polishing fluid corrosion, particle friction, and polishing pad friction[3].

TTV (total thickness variation) is an important metric to characterize the flatness of the wafer surface. The polishing head is one of the most important factors because it directly affects the quality of wafer-polishing. To improve the flatness and uniformity of the wafer surface, M. Liu et al proposed to a 200mm multi-zone (Contour) polish head design to solve the TTV issue that the inability to control edge area[4]. Y. E. Lu et al proposed to distribute the wafer stay time on polishing pad by zones in order to improve the non-uniformity of the pad[5].X.Y Biao et al set up the model of wafer-pad contact pressure distribution using finite element analysis and analyzed the effect of pressurized retainer ring on the pressure distribution[6].

Polishing pressure is a critical factor that affects the quality of polishing. Excessive polishing pressure

can accelerate the wear of the polishing pad, reduce the effectiveness of the polishing liquefaction process, result in uneven material removal, increase surface scratches, and ultimately compromise the quality of the machined surface[7-9]. This effect is particularly evident in the ultra-thin silicon single crystal double-sided polishing process, where polishing fragment rate is primarily affected by the applied polishing pressure. Consequently, precise control of polishing pressure is crucial to achieving high-quality polished surfaces, particularly for delicate materials[10-11]. Thus, in order to achieve high-precision flatness and ultra-thin wafer, the pressure exerted from the polishing head needs to be accuracy controlled.

However, current pressurizing processes for semiconductor polishing equipment, such as pneumatic or self-weight pressurization, can be inadequate for meeting the processing needs of different polishing conditions. Furthermore, the pressure value output by the polishing system is easily affected by various factors, which can result in inconsistent accuracy of the polishing equipment for producing semiconductors.

To overcome the above defects, this paper proposes a methodology for analyzing the uncertainty component of the downward pressure applied to the wafer based on a flexible airbag in a double side polishing machine. By using this approach, all of the parameters involved in the estimation of pressure can be traced back to the international basic unit system (SI), leading to improvements in the reliability of semiconductor polishing equipment.

More specifically, the uncertainty of the downward pressure based on a flexible airbag is calculated via three main steps. (1)A physical model based on the pressure structure of flexible airbag is established, and the formula of the downward pressure is determined. (2) The uncertainty components of the downward pressure based on the formula and the transmission chain of the pressure are obtained, and the correlation analyses of each link in the transmission chain to determine the correlation coefficient between the components of each uncertainty are performed. (3) The factors affecting the pressure in each link are classified, and the synthetic standard uncertainty is calculated according to the components of all uncertainties, and then the synthetic expended uncertainty and the metrological traceability system is obtained[12-14]. The whole process of measurement uncertainty evaluation is shown in Fig.1.

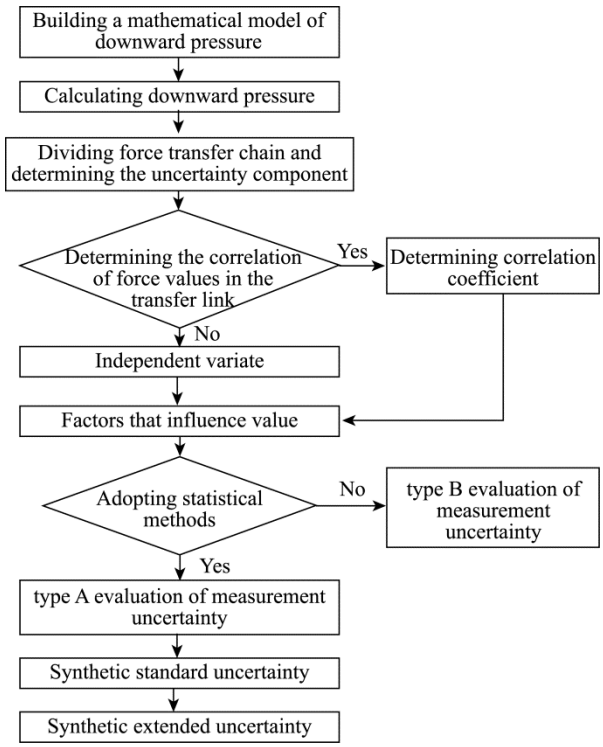

Fig.1 The Process of Downward Pressure Uncertainty Evaluation

2 Method

2.1 Setting up Physical Model Based on the Pressure Structure of Flexible Airbag

The schematic diagram of the polishing machine is shown in Fig.2. The flexible airbags include an upward airbag and a downward airbag. A swing disk is located between both airbags, with one end of the disk connected to a lateral locator, which is fixed to the shell to prevent any lateral swing of the airbag during expansion. The other end of the swing disk is connected to a lever, which facilitates force transfer to a polishing head connected to the end of the lever. A sensor is typically installed between the lever and the polishing head to measure the force value applied to the wafer during the polishing process.

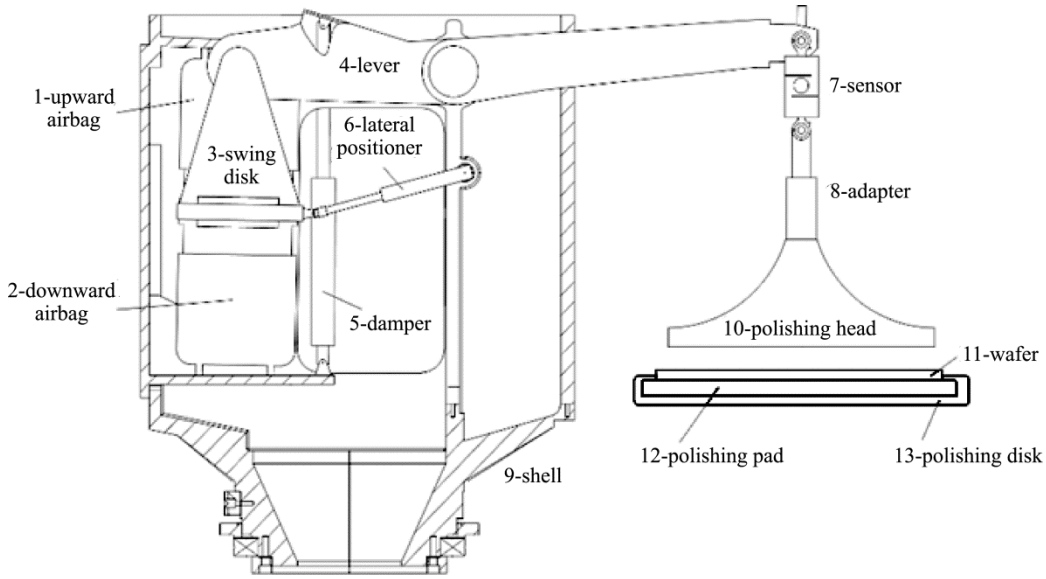

Fig.2 The Schematic Diagram of the Polishing Machine

Fig.3 presents a simplified model of the force value transfer mechanism in the device. Based on this model, we can express the output force value of the polishing head using the following equation:

$$F = k_L * F_{airbag} + F_{head} \tag{1}$$

where F is the value displayed by the sensor, k_L is the ratio of lever, F_{airbag} is the downward pressure caused by the airbag pressurizing, F_{head} is the downward pressure caused by dead weight of the polishing head.

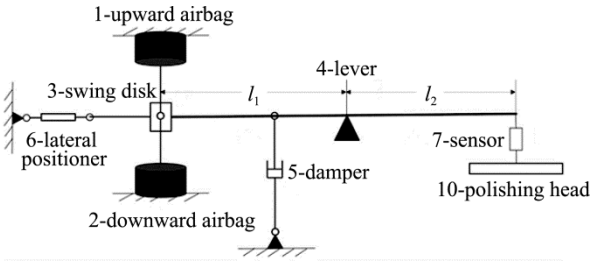

Fig.3 The Simplified Model of Force Value Transfer of the Device

2.2 Setting up Physical Model Based on the Pressure Structure of Flexible Airbag

Based on the information provided in Fig.3, the downward pressure required for batch polishing of wafers is generated by the airbag and polishing head. This pressure is then amplified by a lever and transmitted to the swing disk, polishing head, and the output monitoring system. The force transfer chain of the flexible airbag pressure structure can be divided into five distinct parts which include the airbag pressure system, swing disk, lever system, polishing head system, and output monitoring system.

The total differentiation of formula (1) is carried out. Since k_L、F_{airbag} and F_{head} are relatively independent value, correlation coefficient among these components can be omitted. The relative standard uncertainty u_F of downward pressure can be expressed as follows[15]:

$$u_F = [(\frac{k_L \cdot u_{F_{airbag}}}{F})^2 + (\frac{F_{airbag} \cdot u_{k_L}}{F})^2 + (\frac{u_{F_{head}}}{F})^2 + (u_{swing})^2 + (u_{sensor})^2]^{0.5} \tag{2}$$

where $u_{F_{airbag}}$ is the uncertainty caused by airbag, u_{k_L} is the uncertainty caused by lever, $u_{F_{head}}$ is the uncertainty caused by polishing head, u_{swing} is the relative standard uncertainty caused by swing disk, u_{sensor} is the relative standard uncertainty caused by sensor. The component of downward pressure uncertainty in polishing system as shown in Fig.4.

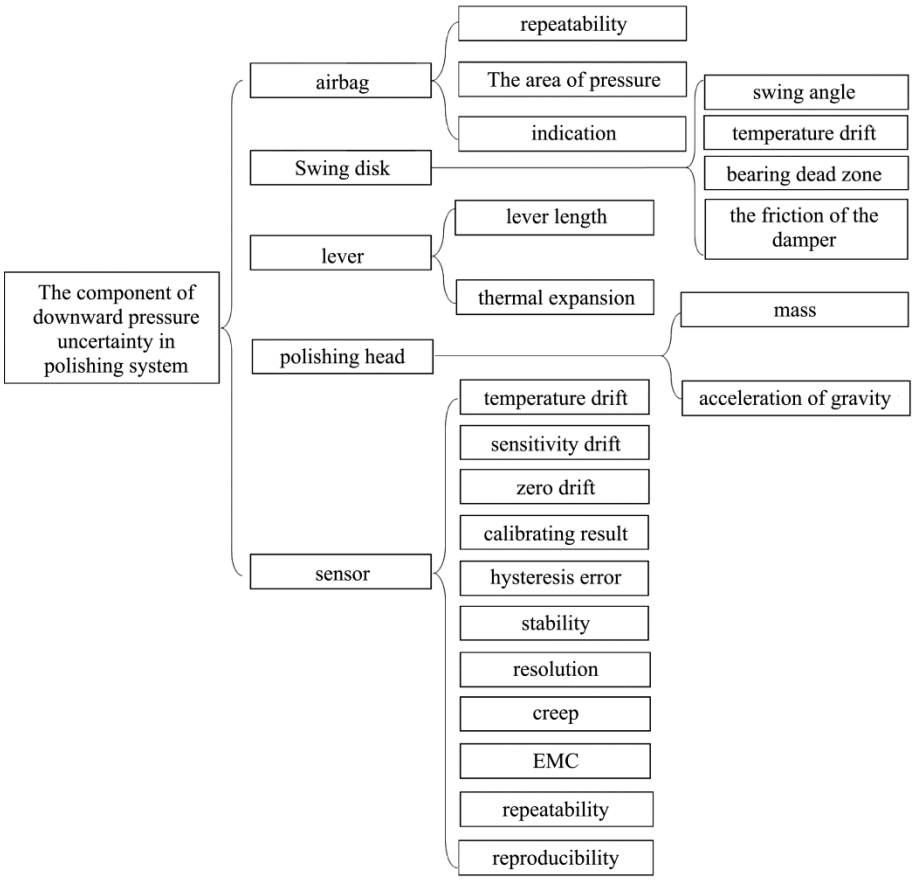

Fig.4 The Component of Downward Pressure Uncertainty in Polishing System

3 Calculating the Component of Uncertainty and Establishing the Metrological Traceability System

3.1 The Uncertainty Caused by Airbag

The calculation formula of airbag downward pressure as follows:

$$F_{airbag} = P_{airbag} \cdot S_{airbag} \tag{3}$$

where P_{airbag} is the pressure of the airbag, and S_{airbag} is the contact area between the airbag and the swing disk. Thus, the uncertainty caused by airbag $u_{F_{airbag}}$ can be expressed as follows:

$$\frac{u_{F_{airbag}}}{F_{airbag}} = \frac{[(u_{P_{airbag}} \cdot S_{airbag})^2 + (u_{S_{airbag}} \cdot P_{airbag})^2]^{0.5}}{F_{airbag}} = \sqrt{(\frac{u_{P_{airbag}}}{P_{airbag}})^2 + (\frac{u_{S_{airbag}}}{S_{airbag}})^2} = \sqrt{(u_{rel-P_{airbag}})^2 + (u_{rel-S_{airbag}})^2} \tag{4}$$

The pressure of the airbag is influenced by air pressure floating, the indication error of pressure gauge and pipeline attenuation. So, the relative uncertainty of airbag pressure $u_{rel-P_{airbag}}$ can be expressed as follows:

$$u_{rel-P_{airbag}} = \left[\left(u_{repeatability} \right)^2 + \left(u_{indication} \right)^2 \right]^{0.5} \tag{5}$$

where $u_{repeatability}$ is the relative uncertainty caused by the error of repeated measurement. It can be calculated by Bessel formula. $U_{indication}$ is the relative uncertainty caused by the error between exerted pressure and calibrated pressure.

The nominal area of contact between the airbag and the swing disk S_{airbag} is influenced by temperature and radius of airbag. The real area of contact as follows:

$$S_{airbag} = \pi R^2 \tag{6}$$

where R is the radius of airbag. So, the relative uncertainty of airbag pressure $u_{rel-S_{airbag}}$ can be

expressed as follows:

$$u_{rel-S_{airbag}} = \left[\left(\frac{\partial S_{airbag}}{\partial T}\cdot\frac{\Delta T}{S_{airbag}}\right)^2+\left(\frac{\partial S_{airbag}}{\partial R}\cdot\frac{\Delta R}{S_{airbag}}\right)^2\right]^{0.5} = \left[\left(\frac{2C}{R}\cdot\Delta T\right)^2+\left(\frac{2\Delta R}{R}\right)^2\right]^{0.5} \quad (7)$$

where T is the current ambient temperature, ΔT is the temperature deviation, and ΔR is the radius deviation, $C=\frac{\partial R}{\partial T}$ is the linear expansion coefficient of temperature.

3.2 The Uncertainty Caused by Swing Disk

The uncertainty caused by swing disk is related to four factors: swing angle θ, temperature T, bearing dead zone and the friction of the damper. The uncertainty u_{swing} can be described as follows:

$$u_{swing} = \left[\left(u_\theta\right)^2+\left(u_T\right)^2+\left(u_{bearing}\right)^2+\left(u_{damper}\right)^2\right]^{0.5} \quad (8)$$

where u_θ is the uncertainty caused by swing angle, u_T is the uncertainty caused by temperature, $u_{bearing}$ is the uncertainty caused by the poor rotation of the bearing in excess of its radial rated load, u_{damper} is the uncertainty caused by the resistance generated by the damper at the beginning of operation.

As shown in Fig.2, the direction of force action is vertical. When there is an angular deviation θ between the actual and ideal direction of the force value, the uncertainty caused by swing angle u_θ can be described as follows:

$$u_\theta = \sqrt{\left(\frac{\partial F_{airbag}}{\partial\theta}\cdot\frac{1}{F_{airbag}}\cdot\frac{1}{\sqrt{3}}\right)^2+(u_\theta')^2} = \sqrt{\left(\frac{1-\cos\theta}{\sqrt{3}}\right)^2+(u_\theta')^2} \quad (9)$$

where u_θ' is the uncertainty of angular calibration, it depends on the superior standards of measurement. The value range of the swing angle θ could be calculated according to the actual maximum free swing. And the probability of the position with swing angle θ of 0 degree is higher than that of the two ends due to the dead weight of the swing disc.

The uncertainty caused by temperature u_T mainly depends on uneven thermal expansion of swing disk structure. Considering the unilateral maximum deformation in the three-dimensional direction, we can obtain:

$$\frac{\partial F}{\partial T}\cdot u_T = \sqrt{\frac{\sum_{i=1}^{3}\left(\frac{\partial f}{\partial x_i}\cdot\frac{\partial x_i}{\partial T}\right)^2}{\sum_{i=1}^{3}x_i^2}}\cdot u_T \quad (10)$$

where $\frac{\partial f}{\partial x_i}\cdot\frac{\partial x_i}{\partial T}$ stands for F in the x_i direction projection force values under the influence of temperature variation.

The uncertainty caused by the poor rotation of the bearing $u_{bearing}$ can be eliminated by matching the actual bearing size with the rated load.

The uncertainty caused by the resistance u_{damper} can be omitted when the loading system is stable, the deformation rate is zero and thus the damping force is almost zero.

3.3 The Uncertainty Caused by Lever

According to lever principle, the ratio of lever k_L can be described as follows:

$$k_L = \frac{l_1}{l_2} \quad (11)$$

where l_1 is the length of the lever arm on the side of F_{airbag}, and l_2 is the length of the lever arm on the side of sensor.

So, the uncertainty caused by lever u_{k_L} can be expressed as follows:

$$u_{k_L} = \left[\left(\frac{u_{l_1}}{l_2}\right)^2+\left(\frac{l_1\cdot u_{l_2}}{l_2^2}\right)^2\right]^{0.5} \quad (12)$$

where u_{l_1} is the uncertainty caused by l_1, u_{l_2} is the uncertainty caused by l_2. The relative standard uncertainty caused by lever arm can be estimated by CMM (Coordinate Measuring Machine): $u_{l_1}=u_{l_2}=10^{-6}$. Since the lever arm l_1 and l_2 are made of the same material, the measurement error due to temperature

expansion can be ignored.

3.4 The Uncertainty Caused by Polishing Head

The uncertainty caused by polishing head $u_{F_{head}}$ is related to mass m_{head} and gravitational acceleration g. So, $u_{F_{head}}$ can be expressed as follows:

$$u_{F_{head}} = \left[\left(u_{m_{head}} \cdot g \right)^2 + \left(u_g \cdot m_{head} \right)^2 \right]^{0.5} \tag{13}$$

3.5 The Uncertainty Caused by Sensor

The sensor consists of high precision pressure two-way force sensor and display panel. The uncertainty caused by sensor is influenced by the following factors: temperature, sensitivity drift, zero drift, calibration result, hysteresis error, resolution, stability, EMC, creep, repeatability and reproducibility. So, the uncertainty caused by sensor can be described as follows:

$$u_{sensor} = (u_{temp}^2 + u_{sendrift}^2 + u_{zerodrift}^2 + u_{cal}^2 + u_{hyst}^2 + u_{st}^2 + u_{resolution}^2 + u_{EMC}^2 + u_{creep}^2 + u_{re}^2 + u_{rp}^2)^{0.5} \tag{14}$$

The uncertainty influenced by temperature u_{temp} can be expressed as follows:

$$u_{temp} = \frac{1}{\sqrt{3}} \cdot \frac{\delta T}{T} \frac{\delta F_T}{F_T} \tag{15}$$

where $\frac{\delta T}{T}$ is the relative variation of temperature, $\frac{\delta F_T}{F_T}$ is the maximum relative variation in force value affected by temperature, it can be obtained by experiments at different temperatures under the same load.

The uncertainty influenced by sensitivity drift $u_{sendrift}$ can be expressed as follows:

$$u_{sendrift} = \frac{1}{\sqrt{3}} \cdot \frac{\delta T}{T} \frac{dS}{dT} \tag{16}$$

where $\frac{\delta T}{T}$ is the relative variation of temperature, $\frac{dS}{dT}$ is the rate of change in sensitivity to temperature.

The uncertainty influenced by zero drift $u_{zerodrift}$ can be expressed as follows:

$$u_{zerodrift} = \frac{1}{\sqrt{3}} \cdot \frac{\delta T}{T} \frac{\delta r}{r} \tag{17}$$

where $\frac{\delta T}{T}$ is the relative variation of temperature, $\frac{\delta r}{r}$ is the maximum rate of change of the zero output as the temperature changes, according to requirements of JJG 391-2009[16].

The uncertainty influenced by calibrating result u_{cal} can be obtained from calibration certificate, which belongs to type B evaluation of measurement uncertainty.

The uncertainty influenced by hysteresis error u_{hyst} can be expressed as follows:

$$u_{hyst} = \frac{1}{\sqrt{3}} \cdot \frac{\delta F_{hyst}}{F_{hyst}} \tag{18}$$

where δF_{hyst} is the maximum difference of indication value between process and return at the same load point, and F_{hyst} is equivalent indication value.

The uncertainty influenced by stability u_{st} can be expressed as follows:

$$u_{st} = \frac{1}{\sqrt{3}} \cdot \frac{\delta F_{st}}{F_{st}} \tag{19}$$

Where δF_{st} is the maximum variation of sensor value obtained from tests at least one-year intervals under the same load and environment conditions. F_{st} is equivalent indication value.

The uncertainty influenced by resolution $u_{resolution}$ can be expressed as follows:

$$u_{resolution} = \frac{1}{2\sqrt{3}} \cdot \frac{\delta R_{res}}{R_{res}} \tag{20}$$

where δR_{res} is the minimum division value, R_{res} is the division value of the current reading.

The uncertainty influenced by EMC u_{EMC} can be expressed as follows:

$$u_{EMC} = \frac{1}{\sqrt{3}} \cdot \frac{\delta R}{R} = \frac{1}{\sqrt{3}} \cdot \sqrt{\sum_{i=1}^{7} \left(\frac{\delta R_i}{R_i} \right)^2} \tag{21}$$

where δR is the indicating value change caused by the change of EMC, and R is the current indicating value.

According to relevant IEC standards, there are seven items to evaluate the electromagnetic interference caused by sensors:

(1) Power voltage variation (DC: IEC 61000-4-29\IEC61000-4-1; AC: IEC 61000-2-1\ IEC61000-4-1)

(2) Short-time power reductions (DC: IEC 61000-4-29\IEC61000-4-1; AC: IEC 61000-4-11\ IEC61000-6-1\6-2)

(3) Bursts (electrical fast transients) (IEC 61000-4-4)

(4) Surge (IEC 61000-4-5)

(5) Electrostatic discharge (IEC 61000-4-2)

(6) Exposure to radiated RF electromagnetic fields (IEC 61000-4-3)

(7) Exposure to conducted currents generated by RF EM fields (IEC 61000-4-6)

The uncertainty influenced by creep u_{creep} can be expressed as follows:

$$u_{creep} = \frac{1}{\sqrt{3}} \cdot \frac{t_{test}}{t_{\max}} \cdot \frac{\delta F_{cr}}{F_{cr}} \tag{22}$$

where $\frac{\delta F_{cr}}{F_{cr}}$ is the relative output of creep, t_{max} is the full-scale loading time of the sensor, t_{test} is time taken to measure the reading.

The uncertainty influenced by repeatability u_{re} can be expressed as follows:

$$u_{re} = \frac{s}{\sqrt{n}} = \sqrt{\frac{\sum_{i=1}^{n}(x_i - \bar{x})^2}{n(n-1)}} \tag{23}$$

where s stands for standard deviation, n is the number of repeated measurements, x_i is the relative indication of the single measurement, and $\bar{x}$ is the average of multiple relative measurement. u_{re} belongs to type A evaluation of measurement uncertainty, which can be obtained by Bessel formula under the condition of multiple calibration in a short time through the sensor.

The uncertainty influenced by reproducibility u_{rp} can be expressed as follows:

$$u_{rp} = \frac{s}{\sqrt{n}} = \sqrt{\frac{\sum_{i=1}^{n}(x_i - \bar{x})^2}{n(n-1)}} \tag{24}$$

where x_i is the relative average of proportional coefficient obtained by single group linear regression, and $\bar{x}$ is the relative average of multiple groups of different orders. u_{rp} belongs to type A evaluation of measurement uncertainty, which can be obtained by Bessel formula under the same control condition of multiple calibration at different times through the sensor.

3.6 The Uncertainty Caused by Sensor

According to the relative size and independent distribution characteristics of each uncertainty component above, the relative extended uncertainty is

$$U_F = k \cdot u_F \tag{25}$$

with k=2, the confidence probability is 95%.

3.7 Establishing the Metrological Traceability System

In order to ensure that any uncertainty in the u_F evaluation process can be traced, Fig.5 shows that each link of the polishing system capable of generating downward pressure corresponds to a specific measurement standard of the national measurement system.

The key physical quantities that make up the pressurized part of the airbag, such as air pressure and size, are traced to the national pressure and length standards respectively. The angle of the swing disk is traced to the national angle standard. The physical quantities that make up the lever system are traced to the national length and angle standards.

The traceability of the polishing head system is ensured through the quality system. The force sensor of the sensor system is traced to the national force standard, while the measurement and analysis of ambient temperature in all links is traced to the national temperature standards.

All of the above national standards are traced to the national standard through quantitative transmission. The physical constant of the basic unit is redefined in accordance with the international metrological system so that the downward pressure of the polishing system can eventually be traced to the basic physical constant.

4 Experimental Analysis and Discussion

The uncertainty caused by airbag is related to P_{airbag} and R. In order to ensure that the polishing head and wafers are fully contact, the pressure P_{airbag} generally takes 0.3-0.8MPa.

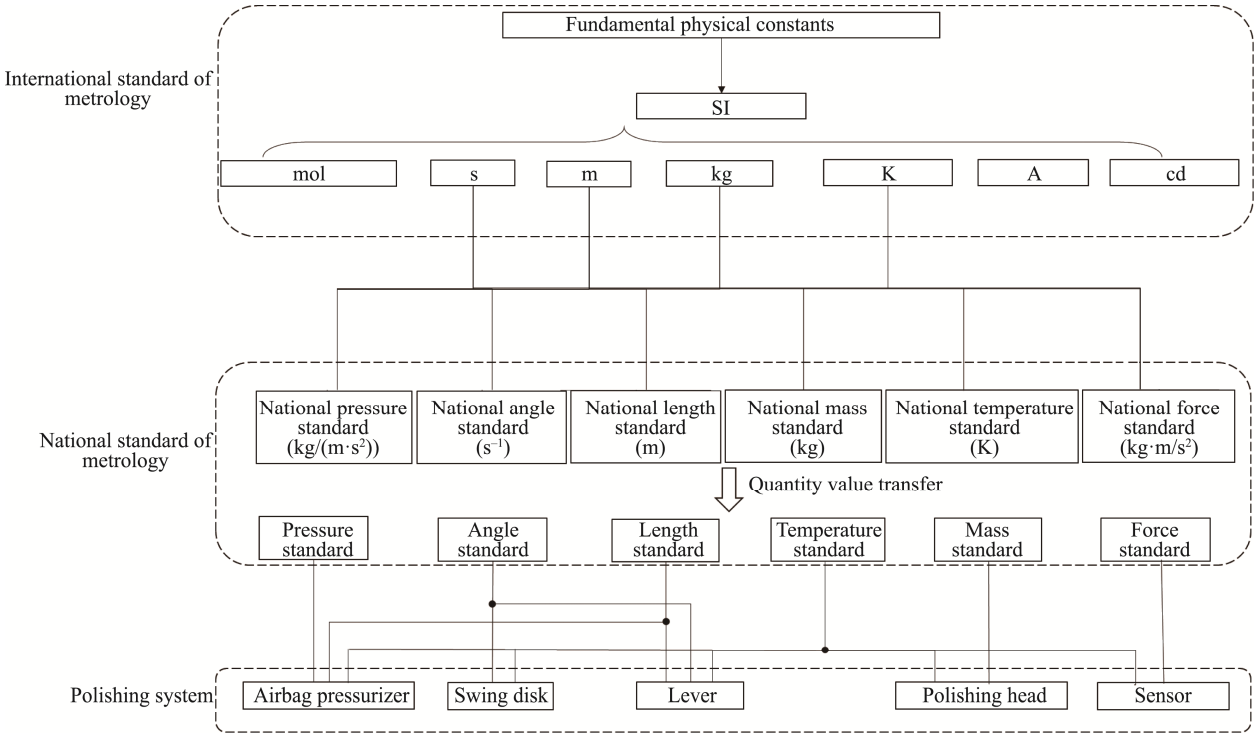

Fig.5 The Traceability System of the Measurement Value

In this experiment, the pressure of airbag P_{airbag}=0.5 MPa, The radius of airbag R=115.00mm, the deviation of radius ΔR=0.1mm. The linear expansion coefficient of temperature C=10^{-5}, ΔT≈2℃. So F_{airbag}=$2.07\times10^{4}N$.

According to repeated measurement, $u_{repeatability}$≈3% and $u_{indication}$≈1%, thus, the relative uncertainty of airbag pressure $u_{rel-P_{airbag}}$=3.162%.

thus, the relative uncertainty of contact area $u_{rel-S_{airbag}}$=0.070%.

So, the relative uncertainty caused by airbag

$$\frac{u_{F_{airbag}}}{F_{airbag}}=\sqrt{(3.162\%)^2+(0.070\%)^2}=3.163\%$$

From physical calibration and 3D model of polishing head, $u_{m_{head}}$=10^{-6}, m_{head}=602kg. By the way of absolute gravity method, u_g=$2\times10^{-7}$and g=9.80N/kg. So, the uncertainty caused by polishing head $u_{F_{head}}/F_{head}$≈0.002%

The uncertainty caused by lever u_{k_L} is related to l_1、l_2、u_{l1} and u_{l2}. u_{l1}=u_{l2}=10^{-6}, l_2=1.5l_1=0.75m, so k_L=$\frac{2}{3}$ and u_{k_L}≈1.60×10^{-6}.

The uncertainty caused by swing disk is consist of swing angle, temperature, bearing dead zone and the friction of the damper. According to the analysis from section 3.2, $u_{bearing}$ and u_{damper} can be omitted by means of control. The error of swing angle is 2° and the deviation of temperature is 2℃. F in the x_i direction relative projection force values under the influence of temperature variation is 0.01%. So u_θ and u_T can be calculated as follows:

$$u_\theta=\frac{1-\cos 2^\circ}{\sqrt{3}}=0.035\%$$

$$u_T=\sqrt{3}\cdot 0.01\%=0.017\%$$

The uncertainty caused by swing disk u_{swing}=0.038%

The pressure sensor used in the device is FT-ZFA-FE-1018. In this sensor, the temperature effect on zero is 0.002%FS/℃, the temperature effect on sensitivity is 0.002%FS/℃. And the temperature effect on indication error is about 0.005%FS/℃. During the whole test, the maximum temperature change is 2℃. So, the uncertainty influenced by sensitivity drift $u_{sendrift}$ and zero-drift $u_{zerodrift}$ are

$$u_{sendrift} = u_{zerodrift} = \frac{1}{\sqrt{3}} \cdot 2 \cdot 0.002\% = 0.0023\%$$

$$u_{temp} = \frac{1}{\sqrt{3}} \cdot 2 \cdot 0.005\% = 0.0058\%$$

the creep error per 30 minutes is 0.02%FS. So, the uncertainty influenced by creep u_{creep} is

$$u_{creep} = \frac{1}{\sqrt{3}} \cdot 0.02\% = 0.012\%$$

The rated voltage output of sensor is 3mV/V, thus the relative resolution of the sensor is 0.3%. the uncertainty influenced by resolution $u_{resolution}$= $\frac{1}{2\sqrt{3}} \cdot 0.3\%$=0.087%

The pressure sensor can be regarded as a standard dynamometer with an accuracy of 0.3. So, the uncertainty influenced by repeatability u_{re} and reproducibility u_{rp} respectively are 0.3%.

The uncertainty influenced by hysteresis error is

$$u_{hyst} = \frac{1}{\sqrt{3}} \cdot 0.3\% = 0.173\%$$

The uncertainty influenced by EMC error is

$$u_{EMC} = \frac{1}{\sqrt{3}} \cdot \sqrt{\sum_{i=1}^{7} \left(\frac{1}{700} \right)^2} = 0.002\%$$

The uncertainty influenced by stable error is

$$u_{st} = \frac{1}{\sqrt{3}} \cdot 0.3\% = 0.173\%$$

The uncertainty influenced by calibrating result u_{cal}=0.15%, which is obtained from calibration certificate.

Thus, according to formula 14, the relative uncertainty caused sensor u_{sensor}≈0.52%.

According to formula 2, the relative uncertainty of downward pressure u_F can be calculated as follows:

$$u_F = [(2.202\%)^2 + (0.001\%)^2 + (0.001\%)^2 + (0.038\%)^2 + (0.52\%)^2]^{0.5} = 2.236\%$$

So, the relative extended uncertainty U_F is

$$U_F = k \cdot u_F = 4.472\%$$

5 Conclusion

In conclusion, this paper presents a novel approach for establishing the traceability of downward pressure uncertainty in wafer polishing machines. The method proposed is highly reliable and accurate, and it has the potential to significantly improve the reliability and consistency of double side polishing machines. According to the experiment of section 4, it can be seen that the pressure of airbag P_{airbag} is the dominate uncertainty component which affects the measurement accuracy. The uncertainty of downward pressure u_F can be decrease by means of using high-precision manometer, improving pressure criteria, reducing loading pressure and lever ratio within appropriate range. This will have a significant impact on the quality of the wafers produced by double side polishing machines, and will help to improve the overall reliability of these machines.

References

[1] Hu, GX. (2007). Research on the double-sided polishing mechanism and process optimization for silicon wafer. M Se. Zhejiang University of Technology.

[2] Wu, MM (2005). Research of the ultraprecision machining techniques of monocrystalline silicon wafer. M Se. Zhejiang University of Technology.

[3] Hu, XZ. (2009). Optimized Design of Ultra-precision Double-sided Polishing Machine. Design and Research, 560(03), pp.54-57.

[4] Liu, M. (2018). Achieving highly accurate profile control by applying a multi-zone polish head for 200mm thin-film SOI CMP. 2018 China Semiconductor Technology International Conference (CSTIC), Shanghai, China, pp. 1-3.

[5] Lu, YE. (2018). CMP pad surface uniformity optimization after polish. 2018 China Semiconductor Technology International Conference (CSTIC), Shanghai, China, pp. 1-4.

[6] Xin, YB. (2000). Modeling of Pad-Wafer Contact Pressure Distribution in Chemical-Mechanical Polishing. 1.

[7] Tang CR. (2016). Simulation Study on Influence Factors of Double Side Polishing Uniformity. M Se. Xiangtan University.

[8] Su, JX. (2005). Analysis of influences on within-wafer-nonuniformity of wafer motion form in wafer chemical mechanical polishing. China Mechanical Engineering, 2005(09), pp.815-818.

[9] Chen, DZ. (1999). Parameter Analysis of Chemical Mechanical Polishing: An Investigation Based on the Pattern Planarization Model. Journal of The Electrochemical Society, 146, pp.3420-3424.

[10] Zhao, Q. (2011). Polishing Process Technology of Ultra-thin Silicon Double Sides Polished Wafer. Equipment for Electronic Products Manufacturing, 40(03), pp.21-23+42.

[11] Yang, WJ. (2011). The Technics of Wafer Ultrathin. Equipment for Electronic Products Manufacturing, 43(04), pp.8-11+37.

[12] Li QZ. (2009). Force Traceability and Evaluation. Engineering & Test, 2009(S1), pp.6-9+53.

[13] Tang. CQ. (2009). Research Development and Summary of Force Measurement Standards. China Measurement & test. 35(03), pp.11-16.

[14] People's Republic of China Standardization Management Committee (2008). JCGM 100:2008. Beijing: Standardization Management Committee, p.1.

[15] Ni. YC. (2014). Practical measurement uncertainty assessment. Beijing: China Standards Press.

[16] People's Republic of China Standardization Management Committee (2009). JJG391-2009. Beijing: Standardization Management Committee, p.1.

Author Biographies

KOU Minghu received B.Sc. degree from Beijing Information Science & Technology University in 2001. He is now the chief technology officer of Beijing TSD Semiconductor Equipment Co., Ltd. His main research interests include grinding and polishing technology of compound semiconductor material.

E-mail: kouminghu@tsd-semicon.com

JIANG Jile received Ph.D. from Tsinghua University in 2012. He is now the chief scientist of Beijing TSD Semiconductor Equipment Co., Ltd. His main research interests include precision measurement, metrology science and tribology, etc.

E-mail: jiangjile@tsd-semicon.com

ZHOU Huiyan received the M.Sc. degree from Tianjin University in 2021. He is now an instrument science researcher in Beijing TSD Semiconductor Equipment Co., Ltd. His main research interests include micro-nano force value calibration and measurement.

E-mail: huiyan9519@tju.edu.cn